Published in final edited form as:

Mol Carcinog. 2017 November ; 56(11): 2474–2485. doi:10.1002/mc.22695.

Secretory Pathway Ca^{2+}-ATPases Promote In Vitro Microcalcifications in Breast Cancer Cells

Donna Dang, **Hari Prasad**, and **Rajini Rao***

Department of Physiology, The Johns Hopkins University School of Medicine, 725 N. Wolfe Street, Baltimore, MD 21205

Abstract

Calcification of the breast is often an outward manifestation of underlying molecular changes that drive carcinogenesis. Up to 50% of all non-palpable breast tumors and 90% of ductal carcinoma *in situ* present with radiographically dense mineralization in mammographic scans. However, surprisingly little is known about the molecular pathways that lead to microcalcifications in the breast. Here, we report on a rapid and quantitative *in vitro* assay to monitor microcalcifications in breast cancer cell lines, including MCF7, MDA-MB-231 and Hs578T. We show that the Secretory Pathway Ca^{2+}-ATPases SPCA1 and SPCA2 are strongly induced under osteogenic conditions that elicit microcalcifications. SPCA gene expression is significantly elevated in breast cancer subtypes that are associated with microcalcifications. Ectopic expression of SPCA genes drives microcalcifications and is dependent on pumping activity. Conversely, knockdown of SPCA expression significantly attenuates formation of microcalcifications. We propose that high levels of SPCA pumps may initiate mineralization in the secretory pathway by elevating luminal Ca^{2+}. Our new findings offer mechanistic insight and functional implications on a widely observed, yet poorly understood radiographic signature of breast cancer.

Keywords

microcalcification; breast cancer; hydroxyapatite; biomineralization; Calcium ATPase; calcium transport; secretory pathway; alizarin red

INTRODUCTION

Microcalcifications are radiographically dense deposits of calcium oxalate or calcium apatite crystals in the soft tissue of breast (1,2). Observed since the early 1900's, microcalcifications are one of the most easily detectable anomalies in a mammogram. Based on their appearance and chemical composition, microcalcifications are classified into two types: Type I are calcium oxalate deposits that are typically associated with benign conditions (3), whereas Type II are composed of bone-like mineralization of hydroxyapatite (4,5). The latter are found in about 40% of primary breast cancers and 90% of ductal carcinoma in situ, where they may be associated with malignancy, bone metastases and poor prognosis. Calcium hydroxyapatite is strongly mitogenic (6), promotes tumor cell migration (7), and has been

*Correspondence: rrao@jhmi.edu.

shown to induce the expression of tumorigenic factors, including matrix metalloproteinases in human breast cancer cell lines (8). Often, microcalcifications are the only mammographic signature of disease, and as a result, it is critically important to understand their underlying etiology. Early detection of harmful microcalcifications and therapeutic intervention could offer novel approaches in the diagnosis and treatment of breast cancers.

Not much is known about the process of microcalcification in breast, and molecular pathways remain poorly understood (2,9). In contrast, a wide range of cellular mechanisms has been implicated in physiological bone mineralization and pathological formation of atherosclerotic plaques (10,11). These include the formation and exocytosis of matrix vesicles loaded with calcium phosphate, exosome release, and direct secretion of non-membrane bound apatite crystals into the extracellular matrix. Common to many of these mechanisms is the role of transporters and enzymes that fuel the accumulation of mineral ions, including Ca^{2+} and Pi. The phosphatase PHOSPHO1 generates phosphates by hydrolysis of phosphocholine and phosphoethanolamine, derived from membrane phospholipids by phospholipase C (12). Alkaline phosphatase (AP) and nucleotide pyrophosphatase phosphodiesterase I (NPP1) have also been implicated in generating inorganic phosphates from organic precursors that are delivered to calcification sites by the Type III Na/Pi co-transporter found on cell and vesicle membranes (12).

Although the obvious importance of Ca^{2+} transporters in formation of breast microcalcifications has been recognized (9), evidence supporting their molecular identity and function is surprisingly lacking. A few Ca^{2+} channels, including annexins (2,13,14) and TRP isoforms (9,15) have been associated with vascular or breast calcifications, respectively. However, passive, downhill Ca^{2+} flux by ion channels is unlikely to play a primary role in the accumulation of Ca^{2+} at microcalcification sites. Therefore, we considered the role of ATP-driven Ca^{2+} pumps that localize to the Golgi and post-Golgi vesicles, belonging to the subgroup of Secretory Pathway Ca^{2+}-ATPases (16,17). In mammary tissue, there are two SPCA pump isoforms that mediate high affinity transport of Ca^{2+} and Mn^{2+} from the cytoplasm to the lumen (18–20). The delivery of these cations to secretory compartments is critical for post-translational protein processing, glycosylation, sorting and quality control (21,22). In the lactating breast, expression of SPCA isoforms is dramatically elevated to facilitate transcytosis of Ca^{2+} from the blood to the lumen of the mammary gland where it accumulates in milk at concentrations of 40–80 mM (23–25). Of particular relevance, an unconventional interaction of SPCA2 with the Ca^{2+} influx channel Orai1, evidenced by co-induction by lactogenic hormones, and co-immunoprecipitation, was required for Ca^{2+} transport in three-dimensional mammosphere cultures (23,26). Gene dysregulation of both SPCA1 (*ATP2C1*) and SPCA2 (*ATP2C2*) has been linked to breast cancers (18): SPCA1 is important for promoting processing of the insulin-like growth factor 1 receptor (IGF-1R), and SPCA2 promotes tumor growth by increasing Ca^{2+} entry through activation of the Orai1 calcium channel (26,27). Thus, we reasoned that the SPCA pumps are likely to be important players in formation of breast microcalcifications.

A major impediment to the identification of novel genes and cellular pathways of microcalcification is a lack of a convenient and quantifiable assay of calcium deposition using well-characterized human breast tumor cell lines. A cocktail of extrinsic factors that

are important for osteogenic differentiation of bone marrow derived mesenchymal stem cells is typically used to elicit mineralization *in vitro* (28,29). This includes (i) dexamethasone, a synthetic glucocorticoid that activates Wnt/beta catenin signaling to augment the effect of bone morphogenetic protein (BMP-2) in a concentration and species dependent manner (30), (ii) ascorbic acid, required as cofactor for enzymes that hydroxylate proline and lysine in procollagen, thereby enhancing the secretion of collagen into the extracellular matrix, and (iii) inorganic phosphate (Pi) or a hydrolysable precursor such as beta-glycerophosphate, for development of hydroxyapatite crystals. An *in vitro* model of mammary cell mineralization was developed using the mouse mammary adenocarcinoma 4T1 cell line, with visible deposits of calcium and phosphate revealed by Alizarin Red and von Kossa staining respectively, beginning at day 11 and continuing through day 28 of culture in osteogenic cocktail (2). Mineralization was not observed with human breast tumor lines, with the exception of a highly metastatic clone of Hs578T that produced hydroxyapatite after 21 days (2). Therefore, a major incentive for this study was to establish assay conditions for shorter and quantifiable measurement of *in vitro* calcium deposition using well characterized and widely used human breast cancer cell models.

We hypothesized that up regulation of secretory pathway Ca^{2+}-ATPases would increase luminal Ca^{2+} in Golgi-derived secretory vesicles and create the appropriate microenvironment for crystallization of calcium and phosphate into hydroxyapatite, in concert with bone mineralization proteins. In this study, we use quantitative *in vitro* measurements of human cancer cell mineralization to evaluate the role of SPCA pumps and provide insight into the process of malignant microcalcifications in breast tissues.

METHODS

Cell lines and Media

MCF10A (ATCC CRL-10317) monolayer cells were cultured in DMEM/F12 containing 5% horse serum, 20ng/ml EGF, 0.5mg/ml hydrocortisone, 100ng/ml cholera toxin, 10μg/ml insulin, and 1X penicillin/streptomycin. MCF7 (ATCC HTB-22) and MDA-MB-231 (ATCC HTB-26) cells were cultured in monolayer with DMEM containing 1X antibiotic/antimycotic, and 10% FBS. Hs578T (ATCC HTB-126) monolayer cells were cultured in DMEM containing 10μg/mL insulin, 1X antibiotic/antimycotic, and 10% FBS. Cells were cultured in 5% CO_2 and at 37°C in a humidified incubator.

Osteogenic Cocktail (OC) and in vitro Cell Mineralization

Cells were cultured in their respective full media supplemented with the OC containing 50μg/ml ascorbic acid (Sigma-Aldrich #A4403), 5–10mM Pi (J.T. Baker #3246-01), 10nM dexamethasone (Sigma-Aldrich #D4902) to induce mineralization. Where noted, BMP2 (PeproTech #120-02) was added to 100–400ng/ml, as specified. Cells were cultured for 3 – 5 days with fresh media every 2 days.

Calcium Solubilization using o-cresolphthalien

After culturing cells in OC media, cells were washed with PBS and were incubated at room temperature in 1M nitric acid for 1 hour. Absorbance was read at 572 nm after treating samples with 0.3 mM o-cresolphthalein and 1M 2-amino-2methyl-1-propanol.

Calcium Staining with Alizarin Red and von Kossa

Cells were cultured on glass coverslips and washed with PBS and fixed in 4% paraformaldehyde for 30 minutes at room temperature. Fixed cells were rehydrated 2 – 3 times and washed 3 times for 5 minutes. For von Kossa staining, coverslips were incubated with 1% silver nitrate (Sigma-Aldrich #209139) under a UV lamp (300nm) for 5 minutes. Coverslips were rinsed 3 times with distilled water and incubated with 5% sodium thiosulfate (Sigma-Aldrich #72049) for 5 minutes to remove any unreacted silver. Cells were stained with Nuclear Fast Red Solution (Sigma-Aldrich #N3020) for 5 minutes and were thoroughly rinsed with distilled water prior to mounting. For Alizarin Red, fixed coverslips were stained with 2%, pH 4.4 Alizarin Red S (7) for 5 minutes and washed 3 times for 5 minutes in PBS and mounted sealed on slides for imaging on an Olympus BX51 DP70 color microscope.

Gene Knockdown and Overexpression

shRNA knockdown constructs and were packaged into the pLK0.1 lentiviral system whereas SPCA2 and SPCA2 D379N rescue constructs were packaged into the FUGW lentiviral backbones. These lentiviruses were produced with pCMV-Δ8.9 and PMDG using a 9:8:1 ratio respectively in HEK293T cells. Following 48 hours, virus was filtered and concentrated using the Lenti-X Concentrator (Clontech #631231). Cells were transfected with lentivirus for 48 hours and selected with 1–2.5μg/ml puromycin for an additional 48 hours. Knockdowns were confirmed by qPCR. All experiments were performed within 5 passages to maintain the knockdown. Expression constructs (empty vector, myc-SPCA1, myc-SPCA2, and FLAG-D379N) were cloned into pcDNA3.1 expression vector and were transiently transfected using Lipofectamine 3000 (Invitrogen #L3000008) according to the manufacturer's protocol.

Real-time Quantitative PCR

RNA was collected and 1μg was used for cDNA synthesis (Applied Biosystems, cat#4387406). The qPCR mastermix was made with EagleTaq Universal Mastermix (Roche, cat#07260296190), 1X Taqman probe, and 50ng of cDNA. The following Taqman probes were utilized: GAPDH (Hs02758991_g1), SPCA2 (Hs00939492_m1), SPCA1 (Hs00995930_m1), BSP2 (Hs00173720_m1), and ALP (Hs02758991_g1).

Western Blot Analysis

Adherent cells were lysed in NP-40 buffer containing protease cocktail inhibitor (Roche cat#11-836-170-001), sonicated, and centrifuged at 14,000rpm for 15 min at 4°C. Lysates were collected and protein concentration was determined using the BCA assay (Thermo cat#23225). 35–50μg of protein was prepared in NuPAGE sample buffer (Invitrogen cat#NP0007) and reducing agent (Ivitrogen cat#NP0004). Proteins were separated on a

SDS-PAGE gel under reducing conditions and were transferred to nitrocellulose membranes (Bio-Rad cat#1620115). The membrane was then blocked in 1% fish gelatin blocking buffer (Amresco cat#M319) at room temperature for 1 hour and primary antibodies (1:1000 Myc-tag (71D10) rabbit monoclonal antibody, Cell Signaling Technology cat#2278; 1:1000 FLAG-tag rabbit polgyclonal antibody, Invitrogen cat#PA1-984B) were applied overnight at 4°C. GAPDH (Sigma cat#G9295) loading control was probed on membranes at 1:20,000 for 1 hour room temperature. SuperSignal West Pico Chemiluminescent Substrate (Thermo cat#34077) was used for detection.

Image Quantification and Statistical Analysis

All raw images were converted to a digitized 8-bit binary image in ImageJ by adjusting the threshold to correct for the background (lower limit: 0, upper limit: 70). The Analyze Particle tool of ImageJ software was utilized to outline each microcalcification and generate counts and areas of outlined particles. Histograms and bar graphs were made using GraphPad Prism and statistical analysis using an unpaired Student's t-test was applied to the quantifications where applicable.

Bioinformatics Analysis

The Cancer Genome Atlas (TCGA) invasive breast carcinoma project datasets were accessed through the cBioPortal (http://www.cbioportal.org/) (31). The microarray data set GSE21422 was analyzed to compare SPCA1 (*ATP2C1*) and SPCA2 (*ATP2C2*) gene expression in control healthy breast, ductal carcinoma in situ (DCIS), and invasive ductal carcinoma (IDC) (n= 19) (32).

RESULTS

Human breast carcinoma cells form microcalcifications *in vitro*

An *in vitro* model for calcification has been achieved by culturing cells in an osteogenic cocktail (OC) containing organic or inorganic phosphate (β-glycerolphosphate or Pi, respectively), ascorbic acid, and the steroid hormone, dexamethasone (33). When combined and cultured with full media, these three components were sufficient to induce visually prominent calcifications, as revealed by Alizarin Red or von Kossa staining, over a period of about 14 – 28 days in murine metastatic mammary 4TI cells (7,33). We wanted to extend these observations to more widely used human breast cancer lines, shorten incubation times and develop more quantifiable results that would be amenable to statistical analysis. In light of recent findings that inorganic phosphate is essential for osteogenic gene expression and differentiation (34,35), and that beta-glycerophosphate causes non-physiological fluctuations in the concentrations of free phosphate (36), we concluded that inorganic phosphate is a more reliable phosphate source in mineralization assays. By replacing β-glycerolphosphate with inorganic phosphate, microcalcifications were observed within 5 days. Here we show Alizarin Red staining of microcalcifications in human breast cancer cell lines, including the estrogen-responsive, ductal carcinoma-derived MCF7 cells, the triple-negative breast cancer line lacking hormone receptors, Hs578T (Figure 1A), and the highly metastatic MDA-MB-231 cell line characterized as claudin-low (Figure S1A). In contrast, no significant mineralization was observed with the nonmalignant, immortalized human mammary

epithelial cell line MCF10A (Figure 1A). The presence of phosphate in the mineral deposits was revealed by von Kossa stain, although staining was relatively weak due to the short incubation period (Figure 1B). No mineralization was observed in the absence of cells, ruling out nonspecific precipitation of salts in culture medium (Figure 1A–B). As expected, fewer microcalcifications were observed in 3 days (Figure S1C), consistent with time-dependent generation of calcium deposits. Examination of images under high magnification (40x) revealed the presence of prominent Alizarin Red staining along cell boundaries in OC supplemented media that was absent in control conditions (Figure S2 A–D).

Quantitative measurement of solubilized calcium using the chromogenic substrate o-cresolphthalein confirmed increases in total calcium of approximately 4-fold and 2-fold in MCF7 cells and Hs578T cells respectively, in OC supplemented media relative to control media conditions. Consistent with Figure 1A, there was no significant change in total calcium levels associated with MCF10A cells upon OC supplementation (Figure 1C).

The shorter generation time resulted in smaller crystals that were amenable to quantitative analysis. In order to more accurately identify microcalcifications and quantify their number and size, Alizarin Red images were digitized and background corrected by adjusting the threshold values to generate binary images as exemplified for MCF7 in Figure 1D. These images were then analyzed using the Particle Counter plug-in in ImageJ to quantify their areas (μm^2) as well as their frequency. As shown by the histograms, a range of microcalcification numbers and sizes could be detected in the human carcinoma cells (Figure 1E and 1F, Figure S1B, D). The observed differences reveal cell type specificity consistent with differing abilities of breast cancer subtypes to form microcalcifications *in vivo*, as discussed ahead.

Next, we assessed whether the calcium deposits observed within this short time frame were related to previously reported microcalcifications. A well known physiological regulator of mineralization is bone morphogenetic protein-2 (BMP2), a secreted protein of the transforming growth factor-β (TGF-β) family that has been implicated as a driver of luminal-type breast cancers (37). Binding of BMP2 to the serine/threonine kinase receptor BMP receptor 1 (BMPR1) activates the downstream phosphorylation pathway of the Smad proteins to induce expression of bone matrix proteins. BMP2 has been shown to induce mineralization of breast tumors in a rodent model *in vivo*, (38,39) and to enhance microcalcifications in mouse mammary 4T1 cells *in vitro* (33). Here, we show that addition of BMP2 results in dose-dependent enhancement of *in vitro* microcalcifications in MCF7 cancer cells (Figure 2A–E). Due to the accelerated time course, supraphysiological levels of BMP2 were most effective, which is not surprising given that calcifications occur over the period of months and years, *in vivo*. Our data suggest that *in vitro* microcalcifications in human breast cancer cells recapitulate physiological mineralization of breast tumors and may be a useful model to determine underlying molecular mechanism.

The Secretory Pathway Ca^{2+}-ATPases, SPCA1 and SPCA2, are upregulated in breast cancer subtypes associated with microcalcifications

Molecular subtyping of breast cancers is important for individualized treatment and disease prognosis. Several studies have established strong correlations between cancer subtype and

the frequency and morphology of mammographically detected microcalcifications. Ductal carcinoma in situ (DCIS) collectively form 15–20% of all breast cancers and are primarily diagnosed by mammography. Strikingly, up to 90% of DCIS present with breast calcifications which may be linear or granular, depending on grade (40). Whereas basal cancers are not associated with calcification (41), luminal A/B types have amorphous deposits with poorly circumscribed margins (42). Mammographic microcalcifications are most likely to be found in HER2-positive breast cancers, where they are large and infiltrating (42–44).

As a first step towards evaluating the role of secretory pathway Ca^{2+} pumps in development of breast microcalcifications, we assessed the expression of SPCA1 and SPCA2 transcripts in mammary cancer subtypes. The housekeeping (i.e., ubiquitously expressed) SPCA1 isoform was modestly, albeit significantly, up regulated in mammary ductal carcinoma *in situ* (DCIS; 1.59-fold higher, $p = 0.0083$; Student's t-test), but not in invasive ductal carcinoma (IDC; $p = 0.24$), relative to healthy control breast samples (Fig. 3A). Notably, SPCA2 transcript was significantly up regulated both DCIS (6.18-fold higher, $p = 0.02$; Student's t-test) and in IDC (6.12-fold higher, $p = 0.03$; Student's t-test) (Fig. 3B)(32). Next, we analyzed sub-type specific expression of SPCA isoforms in 508 breast cancer samples from the TCGA dataset. Whereas high SPCA1 levels were associated with basal subtype of cancer, SPCA2 was significantly elevated in Luminal A/B and HER2+ subtypes ($p<0.001$) that are strongly associated with breast microcalcifications. Whereas both SPCA isoforms may contribute to calcifications observed in DCIS, high expression of SPCA2 appears to be more predictive of breast microcalcifications. These results are intriguing because the two SPCA isoforms share 64% sequence identity and similar ion selectivity and transport properties (18), but show distinct and subtype-specific associations in breast cancer.

SPCA isoforms are induced in osteogenic conditions

Genes involved in the formation of calcifications may show transcriptional changes in response to osteogenic conditions. We observed robust induction of both SPCA isoforms in OC supplemented media, in MCF7 and Hs578T cells. Concomitantly, alkaline phosphatase (ALP) and bone sialoprotein (BSP2) were also induced, as previously reported (7) (Figure 3A–B). Given the paucity of information on transcriptional control of SPCA genes, it was of interest to determine whether induction was mediated by any particular component of OC. We found that addition of individual OC components to growth media failed to elicit increases in SPCA transcripts in MCF7 (not shown), as did combinations of OC components (Figure 3C). Similarly, we failed to observe increases in BSP2 transcript in the absence of complete OC (not shown). Thus, the addition of ascorbic acid, phosphate and dexamethasone is necessary and sufficient for eliciting SPCA transcript increases during microcalcification formation in MCF7 tumor cells.

SPCA1 and SPCA2 promote microcalcification mineralization *in vitro*

We reasoned that SPCA overexpression should enhance Ca^{2+} loading of the Golgi stores, leading to increased Ca^{2+} secretion and promotion of extracellular calcification. To directly test this hypothesis, we transiently overexpressed SPCA1 in MCF7 cells (Figure 5A–C), which have relatively low endogenous expression of this isoform (31). Following culture in

OC supplemented media for 5 days we observed stronger Alizarin Red staining (Figure 5A) and significant increase in number of microcalcifications (Figure 5B) compared with vector-transformed control. Whereas endogenous SPCA2 levels are high in MCF7 cells, expression of this isoform is relatively low in Hs578T cells (31). We show that ectopic expression of SPCA2 in Hs578T cells also significantly enhanced *in vitro* microcalcifications in Hs578T (Figure 5D–F). Previously, SPCA2 was shown to exhibit ATPase-dependent role in sequestering Ca^{2+} into Golgi stores, as well as an unconventional pump-independent role in mediating tumor cell proliferation by eliciting Ca^{2+} influx through plasma membrane ion channels (26). To distinguish between these two roles, we evaluated the effect of a catalytically inactive SPCA2 mutant, D379N, previously shown to lack ATPase and Ca^{2+} pumping activity while retaining normal expression levels and localization (26). Unlike the wild type control, mutant D379N failed to increase mineralization in cells, above that of the empty vector control (Figure 5D–E), showing that formation of calcium deposits in OC-supplemented media by SPCA2 is an active, pump-dependent process.

Loss of SPCA impairs formation of microcalcifications in breast tumor cells

As a further test of a putative role for secretory pathway Ca^{2+}-ATPases in mineralization by tumor cells *in vitro*, we used mixtures of isoform-specific lentivirus-packaged shRNA (26) to knockdown the dominant SPCA isoforms in two breast cancer lines; specifically, SPCA2 in MCF7 (Figure 6A–D) and SPCA1 in Hs578T (Figure 6E–H). Control cells were treated with scrambled shRNA. In the absence of reliable antibodies targeting human SPCA isoforms, we confirmed effective knockdown of target genes using qPCR transcript analysis of transfected cells (Figure 6I). Following transfection and growth to confluency, cells were cultured in OC supplemented media for 5 days. Staining with Alizarin Red and image quantification revealed striking reduction in numbers of microcalcifications upon transcript depletion of either SPCA1 or SPCA2 relative to scramble shRNA treated control in Hs578T and MCF7, respectively. To control for potential off-target effects, shSPCA2 treated MCF7 cells were transfected with silencing-resistant SPCA2 constructs (Figure 6J–K). We show that the number of microcalcifications was restored to control levels by wild type SPCA2, but not by the pump-inactive D378N mutant, confirming the observation of Figure 5D–E. Taken together, these findings reveal, for the first time, a major role for secretory pathway localized Ca^{2+}-ATPases in the formation of microcalcifications in breast cancer cells.

DISCUSSION

Calcification of breast carcinomas is a well-recognized histological and radiographic feature that has been associated with poorer survival in breast cancer patients (1). Although detailed descriptive information is available on the detection, composition and morphology of breast microcalcifications, surprisingly little is known about the underlying cellular pathways. The generation of microcalcifications reflects the biological state of mammary cells, and can provide powerful insight into tumor microenvironment and pathophysiology since breast microcalcifications are correlated with tumor progression and malignancy (45–47). In this context, we have described a fast and quantitative *in vitro* mineralization assay in human breast cancer cells that may be key to deciphering critical players and molecular events leading to formation of microcalcifications.

We show here that the secretory pathway Ca^{2+}-ATPase isoforms, SPCA1 and SPCA2, are important for *in vitro* microcalcifications in human breast cancer cells. We suggest that active, energy dependent pumping of Ca^{2+} ions into the secretory pathway lumen, together with accumulation of anions (phosphate, oxalate) and bone matrix proteins (bone sialoprotein) is necessary for initiation and accumulation of extracellular mineralization (Figure 5). In addition, SPCA2 activates Orai channels at the plasma membrane to elevate cytoplasmic calcium through store-independent calcium entry (SICE), which could drive Golgi and vesicular Ca^{2+} accumulation (26,48). Hydroxyapatite is the main component of malignant microcalcification and it is comprised of Ca^{2+}, Pi, and hydroxide ions (OH^{-}) to form mineral depositions on the collagen I fibers of the extracellular matrix. Although these components can precipitate outside the cell, there is persuasive evidence that breast microcalcifications result from an active cellular process and are not a dystrophic remnant of dead cells. Breast tumor cells have been shown to produce small (20–200 nm) membrane bound vesicles, similar to matrix vesicles produced by calcifying osteoblasts, odontoblasts and chondrocytes (9), within which hydroxyapatite crystals initially deposit. Ultrastructural analysis of breast carcinomas by electron diffraction revealed prominent needle-shaped crystals inside tumor cells, enclosed within cytoplasmic lumina and membrane-bound vesicles, or in gland-like spaces between tumor cells (49).

Recently, it was shown that inhibition of carbonic anhydrase (50) and alkaline phosphatase (6) diminished microcalcification production in mouse 4T1 mammary tumor cells. It has been proposed that calcium channels of the Transient Receptor Potential (TRPC1, TRPM7, TRPV6) and Annexin (A1, A2, A4, A5) families, highly expressed in breast cancer tissues, are responsible for supplying Ca^{2+} to the vesicle lumen for microcalcification formation (9). However, the energy-dependent uphill movement of Ca^{2+} from submicromolar cytoplasmic concentrations into the vesicle lumen is unlikely to be mediated by passive transport mechanisms. Therefore, elucidation of the role of calcium channels in formation of microcalcifications awaits specific knockdown and overexpression approaches as described for the SPCA pumps in this study.

Another key step in the formation of hydroxyapatite crystals in breast tissue is the ectopic expression of bone matrix proteins such as BSP2 by breast cancer cells. Normally expressed by osteoblasts during bone mineralization, secreted glyco/phosphoproteins can bind calcium through their phosphate groups to nucleate the formation of apatite crystals. Furthermore, their ability to bind type I collagen can serve to link the mineral phase to the collagen matrix, and the presence of RGD domains (Arg-Gly-Asp sequence) binds to cell surface integrins and may be important for the preferred bone homing of breast metastases (51,52). The inappropriate expression of bone matrix proteins in breast tumors has been linked to bone metastases, which is significant because breast cancer metastasizes to bone more than any other organ, and over 80% of advanced breast cancer patients develop bone metastases accounting for significant morbidity and mortality (51,52). Breast, prostate and lung cancers are the three most osteotropic of malignant tumors, accounting for 80% of all bone metastases.

Both SPCA isoforms have previously reported roles in breast cancer oncogenesis: SPCA2 elevates cytoplasmic Ca^{2+} to drive proliferation in epithelial-like breast cancers and SPCA1

is important in processing of the insulin-like growth factor 1 receptor (IGF-1R) in basal-like breast cancers (18,26,27). Expression of SPCA2 is high in breast, prostate and lung tissues, whereas SPCA1 has ubiquitous tissue expression (20). Microcalcifications are significantly more prevalent in patients with amplification of the proto-oncogene HER2 (also known as c-erbB2) breast tumors, compared to tumors without amplification of HER2 (43,53,54). It is noteworthy that SPCA2 up regulation is most prominent in ductal carcinomas, and more specifically in HER2 positive breast tumors (18,32). We have shown that high levels of SPCA2 expression in mammary cancers correlate with tumor proliferation and poor survival prognosis (26). These correlative observations, taken together with in vitro evidence from this study strongly suggest that SPCA pumps are a driver of microcalcifications in breast tumors and may offer clinical and physiological insight into the formation of microcalcifications and the tumor microenvironment.

Supplementary Material

Refer to Web version on PubMed Central for supplementary material.

Acknowledgments

Funding: This work was supported by grants from the National Institutes of Health, R01 GM52414 to R.R. We thank Courtney McCann for assistance with preliminary experiments.

Abbreviations

SPCA	Secretory Pathway Calcium ATPase
OC	osteogenic cocktail
Pi	inorganic phosphate
ALP	alkaline phosphatase
BSP	bone sialoprotein
BMP	bone morphogenetic protein

References

1. Morgan MP, Cooke MM, McCarthy GM. Microcalcifications associated with breast cancer: an epiphenomenon or biologically significant feature of selected tumors? Journal of mammary gland biology and neoplasia. 2005; 10:181–187. [PubMed: 16025224]
2. Cox RF, Morgan MP. Microcalcifications in breast cancer: Lessons from physiological mineralization. Bone. 2013; 53:437–450. [PubMed: 23334083]
3. Radi MJ. Calcium oxalate crystals in breast biopsies. An overlooked form of microcalcification associated with benign breast disease. Arch Pathol Lab Med. 1989; 113:1367–1369. [PubMed: 2589947]
4. Sakka E, Prentza A, Koutsouris D. Classification algorithms for microcalcifications in mammograms (Review). Oncology reports. 2006; 15(Spec no):1049–1055. [PubMed: 16525699]
5. Frappart L, Boudeulle M, Boumendil J, Lin HC, Martinon I, Palayer C, Mallet-Guy Y, Raudrant D, Bremond A, Rochet Y, et al. Structure and composition of microcalcifications in benign and malignant lesions of the breast: study by light microscopy, transmission and scanning electron

microscopy, microprobe analysis, and X-ray diffraction. Human pathology. 1984; 15:880–889. [PubMed: 6469237]

6. Morgan MP, Cooke MM, Christopherson PA, Westfall PR, McCarthy GM. Calcium hydroxyapatite promotes mitogenesis and matrix metalloproteinase expression in human breast cancer cell lines. Mol Carcinog. 2001; 32:111–117. [PubMed: 11746823]
7. Cox RF, Hernandez-Santana A, Ramdass S, McMahon G, Harmey JH, Morgan MP. Microcalcifications in breast cancer: novel insights into the molecular mechanism and functional consequence of mammary mineralisation. British journal of cancer. 2012; 106:525–537. [PubMed: 22233923]
8. Cooke MM, McCarthy GM, Sallis JD, Morgan MP. Phosphocitrate inhibits calcium hydroxyapatite induced mitogenesis and upregulation of matrix metalloproteinase-1, interleukin-1beta and cyclooxygenase-2 mRNA in human breast cancer cell lines. Breast Cancer Res Treat. 2003; 79:253–263. [PubMed: 12825860]
9. Sharma T, Radosevich JA, Pachori G, Mandal CC. A Molecular View of Pathological Microcalcification in Breast Cancer. Journal of mammary gland biology and neoplasia. 2016; 21:25–40. [PubMed: 26769216]
10. Ruiz JL, Weinbaum S, Aikawa E, Hutcheson JD. Zooming in on the genesis of atherosclerotic plaque microcalcifications. The Journal of physiology. 2016; 594:2915–2927. [PubMed: 27040360]
11. Golub EE. Biomineralization and matrix vesicles in biology and pathology. Semin Immunopathol. 2011; 33:409–417. [PubMed: 21140263]
12. Orimo H. The mechanism of mineralization and the role of alkaline phosphatase in health and disease. J Nippon Med Sch. 2010; 77:4–12. [PubMed: 20154452]
13. Cmoch A, Strzelecka-Kiliszek A, Palczewska M, Groves P, Pikula S. Matrix vesicles isolated from mineralization-competent Saos-2 cells are selectively enriched with annexins and S100 proteins. Biochemical and biophysical research communications. 2011; 412:683–687. [PubMed: 21867690]
14. Kapustin AN, Davies JD, Reynolds JL, McNair R, Jones GT, Sidibe A, Schurgers LJ, Skepper JN, Proudfoot D, Mayr M, Shanahan CM. Calcium regulates key components of vascular smooth muscle cell-derived matrix vesicles to enhance mineralization. Circ Res. 2011; 109:e1–12. [PubMed: 21566214]
15. Mandavilli S, Singh BB, Sahmoun AE. Serum calcium levels, TRPM7, TRPC1, microcalcifications, and breast cancer using breast imaging reporting and data system scores. Breast Cancer (Dove Med Press). 2012; 2013:1–7. [PubMed: 23662076]
16. Cross BM, Breitwieser GE, Reinhardt TA, Rao R. Cellular calcium dynamics in lactation and breast cancer: from physiology to pathology. Am J Physiol Cell Physiol. 2014; 306:C515–526. [PubMed: 24225884]
17. Sorin A, Rosas G, Rao R. PMR1, a Ca2+-ATPase in yeast Golgi, has properties distinct from sarco/endoplasmic reticulum and plasma membrane calcium pumps. The Journal of biological chemistry. 1997; 272:9895–9901. [PubMed: 9092527]
18. Dang D, Rao R. Calcium-ATPases: Gene disorders and dysregulation in cancer. Biochimica et biophysica acta. 2016; 1863:1344–1350. [PubMed: 26608610]
19. Reinhardt TA, Filoteo AG, Penniston JT, Horst RL. Ca(2+)-ATPase protein expression in mammary tissue. Am J Physiol Cell Physiol. 2000; 279:C1595–1602. [PubMed: 11029307]
20. Vanoevelen J, Dode L, Van Baelen K, Fairclough RJ, Missiaen L, Raeymaekers L, Wuytack F. The secretory pathway Ca2+/Mn2+-ATPase 2 is a Golgi-localized pump with high affinity for Ca2+ ions. The Journal of biological chemistry. 2005; 280:22800–22808. [PubMed: 15831496]
21. Durr G, Strayle J, Plemper R, Elbs S, Klee SK, Catty P, Wolf DH, Rudolph HK. The medial-Golgi ion pump Pmr1 supplies the yeast secretory pathway with Ca2+ and Mn2+ required for glycosylation, sorting, and endoplasmic reticulum-associated protein degradation. Mol Biol Cell. 1998; 9:1149–1162. [PubMed: 9571246]
22. Xiang M, Mohamalawari D, Rao R. A novel isoform of the secretory pathway Ca2+,Mn(2+)-ATPase, hSPCA2, has unusual properties and is expressed in the brain. The Journal of biological chemistry. 2005; 280:11608–11614. [PubMed: 15677451]

23. Cross BM, Hack A, Reinhardt TA, Rao R. SPCA2 regulates Orai1 trafficking and store independent Ca2+ entry in a model of lactation. PLoS One. 2013; 8:e67348. [PubMed: 23840669]
24. Reinhardt TA, Horst RL. Ca2+-ATPases and their expression in the mammary gland of pregnant and lactating rats. Am J Physiol. 1999; 276:C796–802. [PubMed: 10199809]
25. Reinhardt TA, Lippolis JD. Mammary gland involution is associated with rapid down regulation of major mammary Ca2+-ATPases. Biochemical and biophysical research communications. 2009; 378:99–102. [PubMed: 19000904]
26. Feng M, Grice DM, Faddy HM, Nguyen N, Leitch S, Wang Y, Muend S, Kenny PA, Sukumar S, Roberts-Thomson SJ, Monteith GR, Rao R. Store-independent activation of Orai1 by SPCA2 in mammary tumors. Cell. 2010; 143:84–98. [PubMed: 20887894]
27. Grice DM, Vetter I, Faddy HM, Kenny PA, Roberts-Thomson SJ, Monteith GR. Golgi calcium pump secretory pathway calcium ATPase 1 (SPCA1) is a key regulator of insulin-like growth factor receptor (IGF1R) processing in the basal-like breast cancer cell line MDA-MB-231. The Journal of biological chemistry. 2010; 285:37458–37466. [PubMed: 20837466]
28. Langenbach F, Handschel J. Effects of dexamethasone, ascorbic acid and beta-glycerophosphate on the osteogenic differentiation of stem cells in vitro. Stem Cell Res Ther. 2013; 4:117. [PubMed: 24073831]
29. Boskey AL, Roy R. Cell culture systems for studies of bone and tooth mineralization. Chem Rev. 2008; 108:4716–4733. [PubMed: 18800815]
30. Diefenderfer DL, Osyczka AM, Garino JP, Leboy PS. Regulation of BMP-induced transcription in cultured human bone marrow stromal cells. J Bone Joint Surg Am. 2003; 85-A(Suppl 3):19–28.
31. Cancer Genome Atlas, N. Comprehensive molecular portraits of human breast tumours. Nature. 2012; 490:61–70. [PubMed: 23000897]
32. Kretschmer C, Sterner-Kock A, Siedentopf F, Schoenegg W, Schlag PM, Kemmner W. Identification of early molecular markers for breast cancer. Mol Cancer. 2011; 10:15. [PubMed: 21314937]
33. Cox RF, Jenkinson A, Pohl K, O'Brien FJ, Morgan MP. Osteomimicry of mammary adenocarcinoma cells in vitro; increased expression of bone matrix proteins and proliferation within a 3D collagen environment. PLoS One. 2012; 7:e41679. [PubMed: 22911843]
34. Beck GR Jr. Inorganic phosphate as a signaling molecule in osteoblast differentiation. J Cell Biochem. 2003; 90:234–243. [PubMed: 14505340]
35. Beck GR Jr, Zerler B, Moran E. Phosphate is a specific signal for induction of osteopontin gene expression. Proceedings of the National Academy of Sciences of the United States of America. 2000; 97:8352–8357. [PubMed: 10890885]
36. Schack LM, Noack S, Winkler R, Wissmann G, Behrens P, Wellmann M, Jagodzinski M, Krettek C, Hoffmann A. The Phosphate Source Influences Gene Expression and Quality of Mineralization during In Vitro Osteogenic Differentiation of Human Mesenchymal Stem Cells. PLoS One. 2013; 8:e65943. [PubMed: 23823126]
37. Chapellier M, Maguer-Satta V. BMP2, a key to uncover luminal breast cancer origin linked to pollutant effects on epithelial stem cells niche. Mol Cell Oncol. 2016; 3:e1026527. [PubMed: 27314065]
38. Liu F, Misra P, Lunsford EP, Vannah JT, Liu Y, Lenkinski RE, Frangioni JV. A dose- and time-controllable syngeneic animal model of breast cancer microcalcification. Breast Cancer Res Treat. 2010; 122:87–94. [PubMed: 19760034]
39. Liu F, Bloch N, Bhushan KR, De Grand AM, Tanaka E, Solazzo S, Mertyna PM, Goldberg N, Frangioni JV, Lenkinski RE. Humoral bone morphogenetic protein 2 is sufficient for inducing breast cancer microcalcification. Mol Imaging. 2008; 7:175–186. [PubMed: 19123988]
40. Evans A. The diagnosis and management of pre-invasive breast disease: radiological diagnosis. Breast cancer research: BCR. 2003; 5:250–253. [PubMed: 12927034]
41. Cho N. Molecular subtypes and imaging phenotypes of breast cancer. Ultrasonography. 2016; 35:281–288. [PubMed: 27599892]
42. Cen D, Xu L, Li N, Chen Z, Wang L, Zhou S, Xu B, Liu CL, Liu Z, Luo T. BI-RADS 3-5 microcalcifications can preoperatively predict breast cancer HER2 and Luminal a molecular subtype. Oncotarget. 2017; 8:13855–13862. [PubMed: 28099938]

43. Seo BK, Pisano ED, Kuzimak CM, Koomen M, Pavic D, Lee Y, Cole EB, Lee J. Correlation of HER-2/neu overexpression with mammography and age distribution in primary breast carcinomas. Acad Radiol. 2006; 13:1211–1218. [PubMed: 16979070]
44. Patel TA, Puppala M, Ogunti RO, Ensor JE, He T, Shewale JB, Ankerst DP, Kaklamani VG, Rodriguez AA, Wong ST, Chang JC. Correlating mammographic and pathologic findings in clinical decision support using natural language processing and data mining methods. Cancer. 2017; 123:114–121. [PubMed: 27571243]
45. Baker R, Rogers KD, Shepherd N, Stone N. New relationships between breast microcalcifications and cancer. British journal of cancer. 2010; 103:1034–1039. [PubMed: 20842116]
46. Tabar L, Tony Chen HH, Amy Yen MF, Tot T, Tung TH, Chen LS, Chiu YH, Duffy SW, Smith RA. Mammographic tumor features can predict long-term outcomes reliably in women with 1-14-mm invasive breast carcinoma. Cancer. 2004; 101:1745–1759. [PubMed: 15386334]
47. Thurfjell E, Thurfjell MG, Lindgren A. Mammographic finding as predictor of survival in 1-9 mm invasive breast cancers. worse prognosis for cases presenting as calcifications alone. Breast Cancer Res Treat. 2001; 67:177–180. [PubMed: 11519866]
48. Smaardijk S, Chen J, Wuytack F, Vangheluwe P. SPCA2 couples Ca2+ influx via Orai1 to Ca2+ uptake into the Golgi/secretory pathway. Tissue Cell. 2016
49. Ahmed A. Calcification in human breast carcinomas: ultrastructural observations. J Pathol. 1975; 117:247–251. [PubMed: 1214193]
50. Zheng Y, Xu B, Zhao Y, Gu H, Li C, Wang Y, Chang X. CA1 contributes to microcalcification and tumourigenesis in breast cancer. BMC Cancer. 2015; 15:679. [PubMed: 26459317]
51. Waltregny D, Bellahcene A, de Leval X, Florkin B, Weidle U, Castronovo V. Increased expression of bone sialoprotein in bone metastases compared with visceral metastases in human breast and prostate cancers. J Bone Miner Res. 2000; 15:834–843. [PubMed: 10804012]
52. Ibrahim T, Leong I, Sanchez-Sweatman O, Khokha R, Sodek J, Tenenbaum HC, Ganss B, Cheifetz S. Expression of bone sialoprotein and osteopontin in breast cancer bone metastases. Clin Exp Metastasis. 2000; 18:253–260. [PubMed: 11315099]
53. Naseem M, Murray J, Hilton JF, Karamchandani J, Muradali D, Faragalla H, Polenz C, Han D, Bell DC, Brezden-Masley C. Mammographic microcalcifications and breast cancer tumorigenesis: a radiologic-pathologic analysis. BMC Cancer. 2015; 15:307. [PubMed: 25896922]
54. Wang Y, Ikeda DM, Narasimhan B, Longacre TA, Bleicher RJ, Pal S, Jackman RJ, Jeffrey SS. Estrogen receptor-negative invasive breast cancer: imaging features of tumors with and without human epidermal growth factor receptor type 2 overexpression. Radiology. 2008; 246:367–375. [PubMed: 18180338]

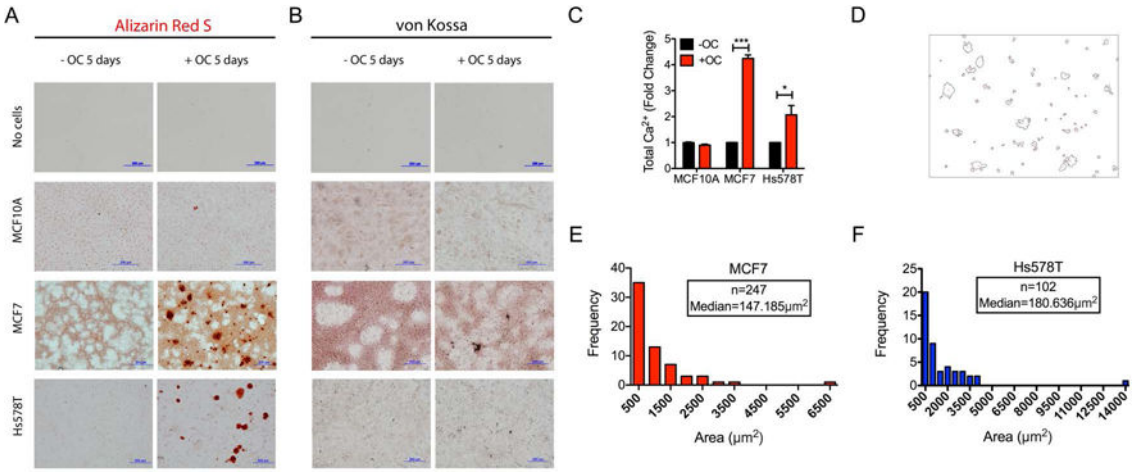

Figure 1. Microcalcifications in cultured breast cancer tumor cells

(A) MCF10A, MCF7, and Hs578T cells were grown to confluency, then cultured for 5 days with or without OC supplemented media before staining with Alizarin Red S. Scale bar = 200 μm, n=3. No cell controls are included in the top panel. (B) MCF10A, MCF7, and Hs578T cells were cultured as described in (A) and stained with von Kossa. Scale bar = 200 μm, n=3. No cell controls are included in the top panel. (C) Cells were cultured as described in (A), then total Ca^{2+} was solubilized with nitric acid and quantified using the o-cresolphthalein colorimetric assay as described in Methods. *p<0.05, ***p<0.001, Student's t-test, n=3. (D) Digitized binary image of Alizarin Red stained MCF7 cells treated with OC supplemented media (shown in A), using ImageJ. (E) Frequency of microcalcifications binned according to size in 500 μm^2 increments from the digitized binary images of MCF7 cells as shown in (D). (F) Frequency of microcalcifications in Hs578T cells as described in (D).

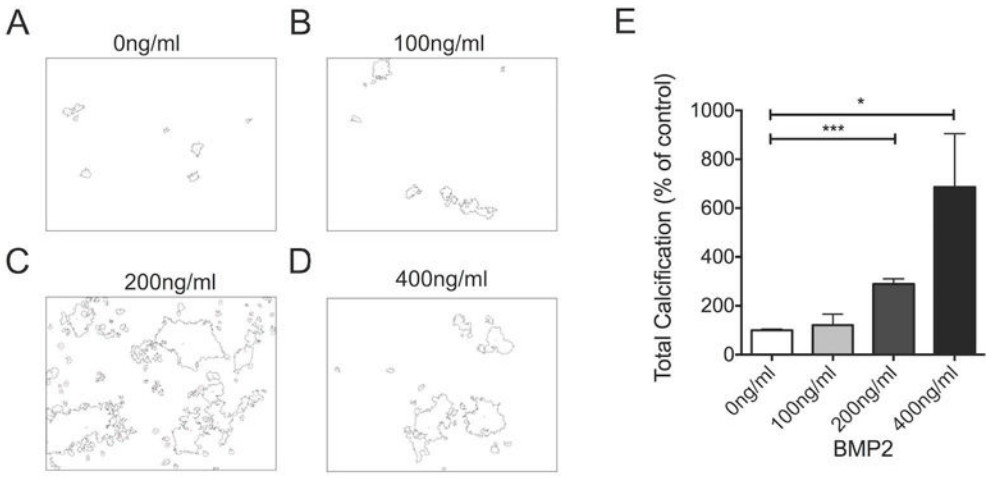

Figure 2. Effect of BMP2 on *in vitro* mineralization

MCF7 cells were grown to confluency and cultured with OC supplemented media in the absence (A) or presence (B-D) of human recombinant BMP2 at the indicated concentrations, for 5 days. After staining with Alizarin Red, images were digitized (A-D). Total calcification (E) was calculated by summing areas defined by the digitized binary images, and expressed as percentage of control lacking BMP2.

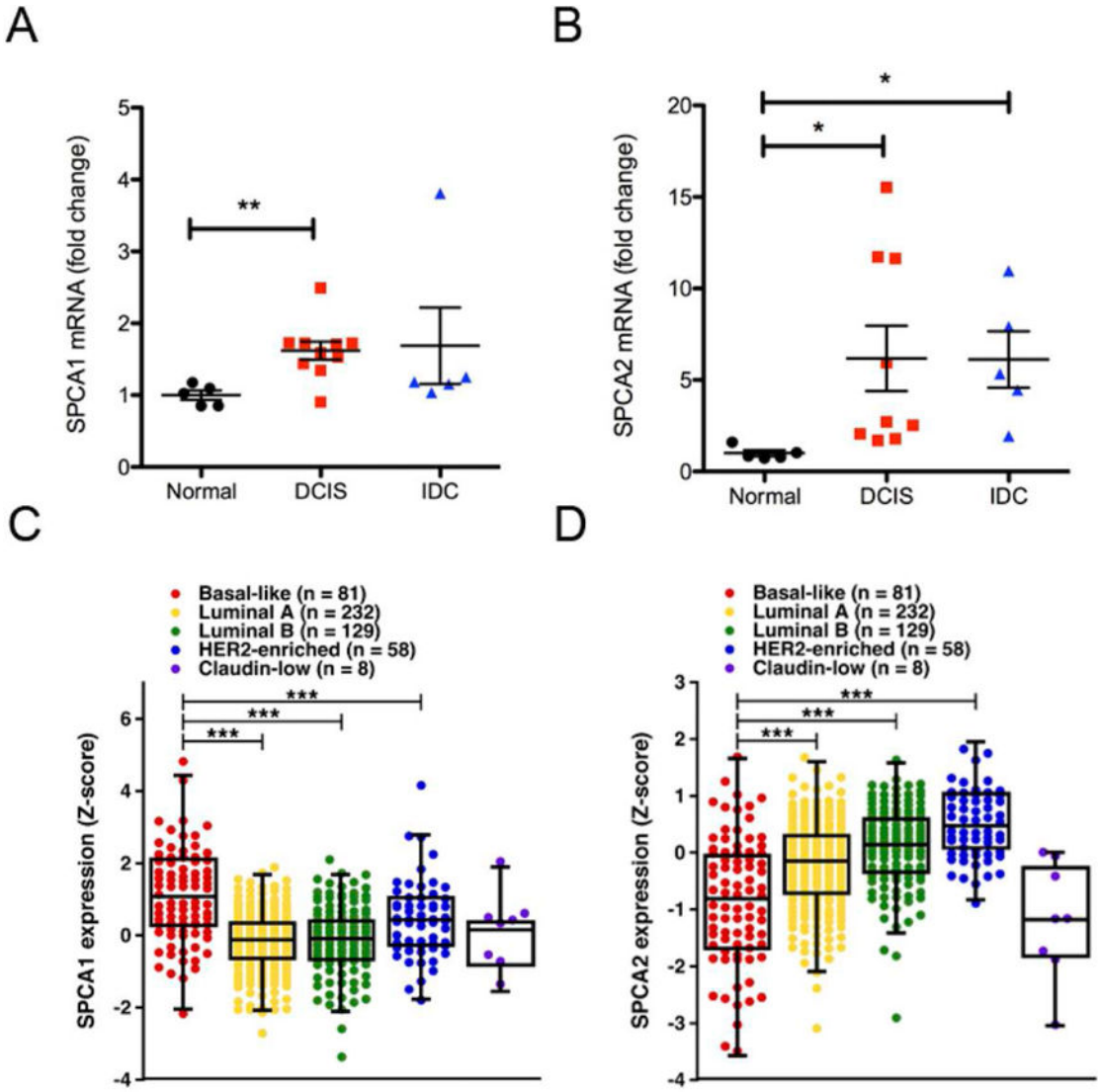

Figure 3. Subtype-specific expression of SPCA isoforms in breast cancer tumors

(A) mRNA expression of SPCA1 levels in ductal carcinoma *in situ* (DCIS) and in invasive ductal carcinomas (IDC) normalized to normal patient tissue from the GSE1422 data set. **p<0.01, Student's t-test, normal n=5, DCIS n=10, IDC n=5. (B) mRNA expression of SPCA2 levels in ductal carcinoma *in situ* (DCIS) and in invasive ductal carcinomas (IDC) normalized to normal patient tissue from the GSE1422 data set(32). *p<0.05, Student's t-test, normal n=5, DCIS n=9, IDC n=5. (C) Subtype-specific gene expression of SPCA1 in tumors from The Cancer Genome Atlas (TCGA); ***p<0.001, Student's t-test. (D) Subtype-specific gene expression of SPCA2 in tumors from TCGA(31); ***p<0.001, Student's t-test.

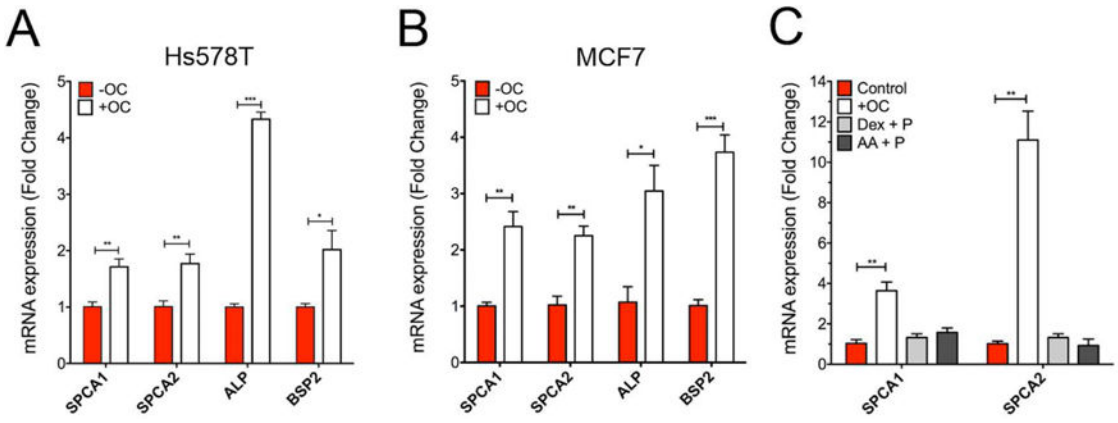

Figure 4. Osteomimetic induction of SPCA pumps in breast cancer mineralization

(A) Hs578T cells were grown to confluency and cultured for 5 days with or without OC supplemented media. RNA was collected from biological triplicates and cDNA was synthesized. qPCR was performed for SPCA1 (**p<0.01, Student's t-test, n=3), SPCA2 (**p<0.01, Student's t-test, n=3), ALP (***p<0.0001, Student's t-test, n=3), and BSP2 (*p<0.05, Student's t-test, n=3). (B) MCF7 cells were grown and treated as in (A). qPCR was performed for SPCA (**p<0.01, Student's t-test, n=3), SPCA2 (**p<0.01, Student's t-test, n=3), ALP (*p<0.05, Student's t-test, n=3), and BSP2 (***p<0.001, Student's t-test, n=3). (C) MCF7 cells were grown to confluency and cultured for 5 days in various media supplemented with two or more components of OC as indicated: dexamethasone (Dex), ascorbic acid (AA), and inorganic phosphate (P). RNA was collected from biological triplicates and cDNA was synthesized. qPCR was performed for SPCA1 (**p<0.01, Student's t-test, n=3) and SPCA2 (**p<0.01, Student's t-test, n=3).

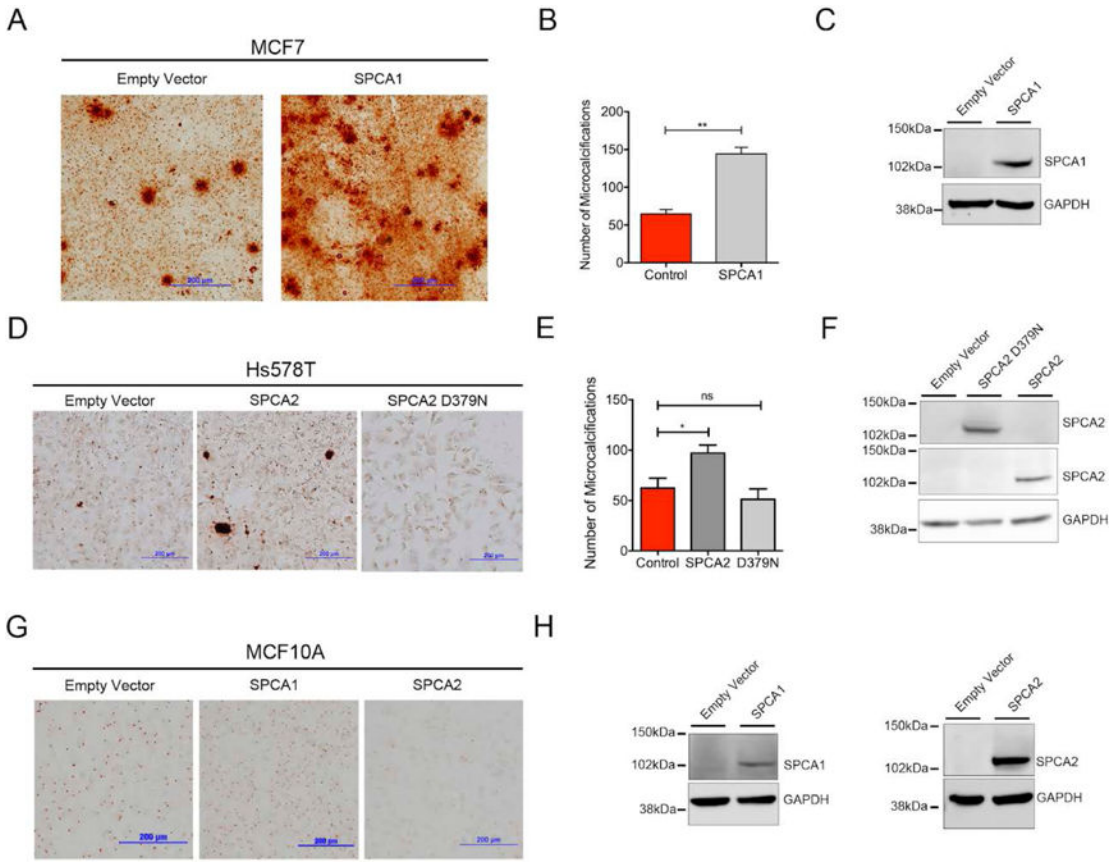

Figure 5. Functional expression of SPCA pumps increases microcalcifications

(A) MCF7 cells were transfected with empty vector (pcDNA plasmid) or SPCA1 gene. Cells were cultured with and without OC supplemented media upon confluency post transfection for 5 days. Cells were then fixed and stained with Alizarin Red and imaged. (B) The number of microcalcifications for each field was quantified for each condition. **p<0.01, Student's t-test, n=3. (C) Western blot showing ectopic expression of SPCA1 in MCF7 cells. (D) Hs578T cells were transfected with pcDNA plasmids containing an empty vector, SPCA2, or SPCA2 D379N. Cells were cultured with and without OC supplemented media upon confluency post transfection for 5 days. Cells were then fixed, stained with Alizarin Red, and imaged. (E) The number of microcalcifications was quantified for each condition. *p<0.05, ns p>0.05, Student's t-test, n=3. (F) Western blot of Hs578T cell lysates showing ectopic expression of wild type SPCA2 and SPCA2 D378N mutant, as described in Methods. (G) MCF10A cells were transfected with pcDNA plasmids containing empty vector, SPCA1, or SPCA2. Cells were cultured with and without OC supplemented media upon confluency post transfection for 5 days. Cells were then stained with Alizarin Red and imaged. (H) Western blot of MCF10A cell lysates showing ectopic expression of SPCA1 and SPCA2.

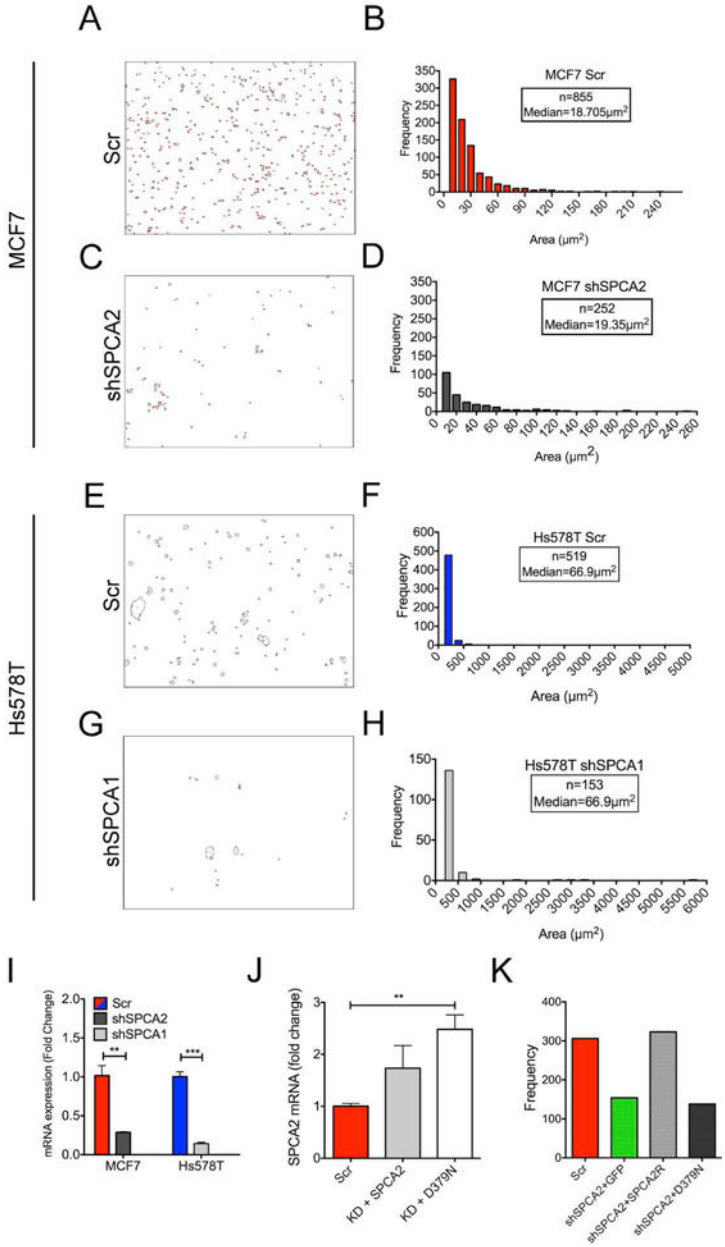

Figure 6. Effect of SPCA gene knockdown on breast cancer microcalcifications

MCF7 cells treated with scrambled (A-B), shSPCA2 (C-D), and Hs578T cells were treated with scrambled (E-F) or shSPCA1 (G-H) lentiviral constructs, then cultured in OC supplemented media post confluency for 5 days. Cells were stained with Alizarin Red S, and the digitized images (A, C, E and G) were analyzed for the number and size of microcalcifications (B, D, F and H) as described in Methods. Microcalcifications were binned by 10 μm^2 (MCF7 scrambled control and shSPCA2 cells) or 200 μm^2 (Hs578T scrambled control cells) or 300 μm^2 (shSPCA1 cells) increments. Knockdown of SPCA isoforms was confirmed by qPCR (I); **p<0.01 and ***p<0.001, Student's t-test, n=3 for each condition. MCF7 cells treated with shSPCA2 were transfected with wild type or

D379N silencing-resistant SPCA2 constructs. Transcripts were monitored by qPCR (J) and microcalcifications were quantified as described above (K); **p<0.01, Student's t-test.

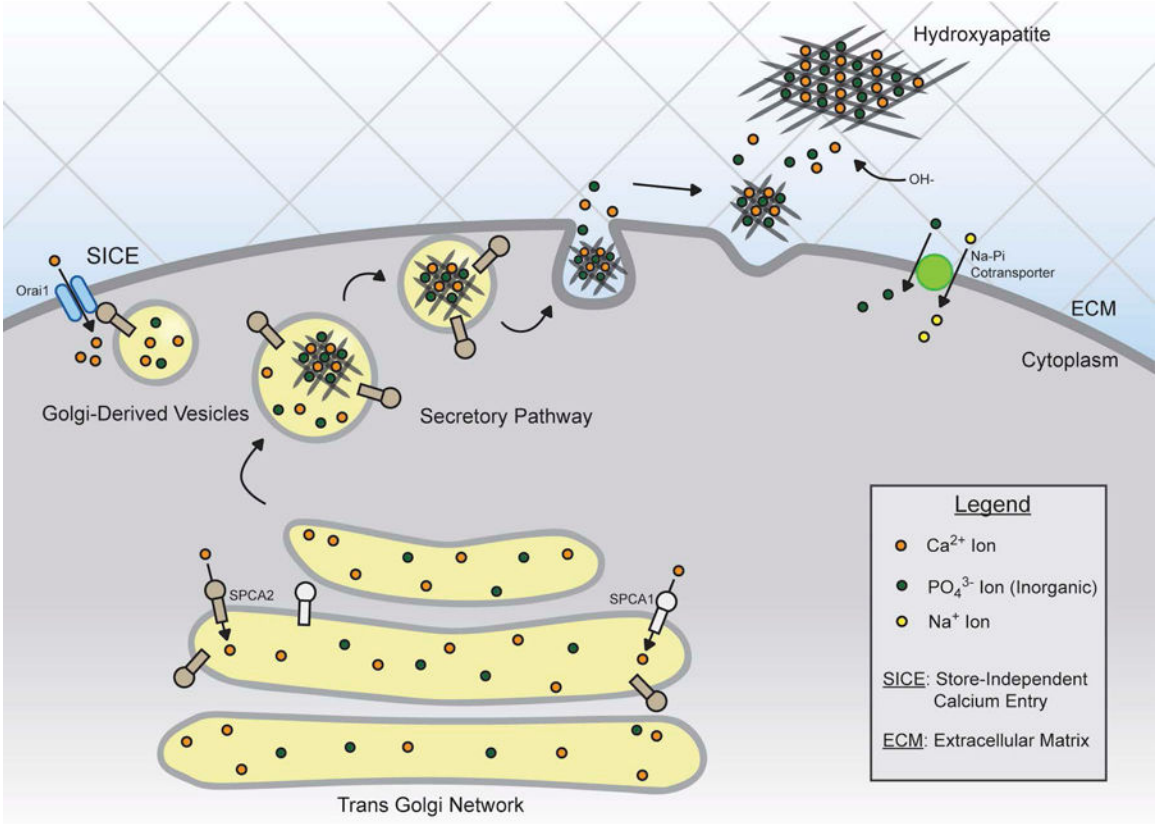

Figure 7. Vesicular calcium sequestration in microcalcification

This schematic proposes a role for SPCA pumps in Ca^{2+} loading of Golgi-derived vesicles in microcalcification of breast tumor cells. Pi can enter the cell through the Na-Pi cotransporter and can be shuttled into organelles. Whereas both SPCA isoforms function to concentrate Ca^{2+} into the Golgi and secretory vesicles, only SPCA2 activates store-independent calcium entry (SICE) through the Orai1 Ca^{2+} channel. Accumulation of Ca^{2+} and Pi ions leads to precipitation of hydroxyapatite crystals inside vesicles. The vesicles are trafficked to the plasma membrane to be released to the extracellular matrix (ECM) where the ions can react with exogenous hydroxide ions (OH^{-}) to form microcalcifications. These crystals, together with bone matrix proteins, lay down a foundation for mineralization.